Zero-Pressure Balloon Design

David L. Keese*
Texas A&M University, College Station, Texas

In atmospheric balloon research it is very important to describe accurately the balance of forces applied to a film and to use this analytical description to produce a suitable manufactured balloon shape. This paper investigates several additions to the presently accepted method for free balloon design. This includes a study of the nonuniform stress state created by the inclusion of load tapes in the theoretical model. The effects of balloon material properties and deformations are also considered. These refinements result in a more accurate theoretical model and an improved design for atmospheric balloons.

Nomenclature

a = distance of the point of zero-pressure differential below the bottom of the balloon
A = balloon surface area
b = specific buoyancy of lifting gas
E_x = film modulus in x direction
k = constant, $(2\pi)^{-1/3}$
K = tape stiffness (force)
n = number of load tapes
p = pressure
P = total balloon payload
r = radius
s = distance measured along a gore
t = film thickness
T = total force
V = balloon volume
w_f = film weight per unit area
w_t = tape weight per unit length
z = height
ϵ_f = film strain
ϵ_t = tape strain
θ = angle between balloon film and the vertical axis of symmetry
λ = normalizing length $(P/b)^{1/3}$
σ_c = circumferential film stress resultant (force/length)
σ_m = meridional film stress resultant (force/length)

I. Introduction

ATMOSPHERIC balloon research is a relatively young and often overlooked area of engineering science. However, the origins of the basic ideas relating to ballooning can be traced through history to before the time of Christ. In 240 B.C. Archimedes stated that a statically floating body must displace its own weight of the fluid in which it floats.[1] The practical application of this principle to balloon flight was not to come until many years later when the Montgolfier brothers constructed several hot-air balloons in the late 1700's. In 1783, hydrogen was first used by Charles and Robert as an improved lifting gas.[1] Prior to this point in history and for approximately 150 years thereafter, the entire range of knowledge in balloon design and construction consisted of only a few simple "rule-of-thumb" concepts. It was not until the late 1930's that the University of Minnesota began an extensive study of atmospheric balloons. This program, prompted by the failure of the first Explorer flight, produced several notable achievements: 1) lightweight plastics were considered for use in the constuction of the gas barrier and 2) a balloon shape and stress analysis was introduced.

This work done by the University of Minnesota marked the beginning of modern atmospheric balloon research. The state-of-the-art in balloon design was advanced further through the work done by Upson and later by Smalley. In his study the equilibrium balance of forces acting on the balloon film was investigated and used to derive a set of equations defining the shape of a specific balloon.[2] These equations have become the accepted basis of modern balloon design in recent years. Research continues at several institutions in such areas as material property investigation and design and analysis of various balloon systems.

As is typical in any growing area of engineering and science, increased demands are encountered which can only be satisfied by a continually improved subject knowledge. This is true of the field of atmospheric balloon research as well. More stringent design criteria demand a more accurate theoretical description of reactions in the balloon film and a more precise design procedure. The main purpose of this paper is to investigate improvements in this area relating to load tape effects and material properties and deformations.

II. Theory

The main goal in atmospheric balloon design is to be able to define a specific balloon shape for the manufacturer which will accurately satisfy a particular set of mission requirements. The presently accepted method by which this is done was developed by Smalley.[2] This procedure determines the characteristics of various balloon shapes through the solution of a set of differential equations. These equations are developed by considering the forces acting on a differential film element of a balloon symmetrically deployed in the float configuration. The boundaries of this element of balloon film are defined in Fig. 1. The film is then considered to be in equilibrium with the forces acting on it as shown in Fig. 2. By summation of the forces in both the meridional and radial directions, the equilibrium equations are found to be:

$$T_{m2}\cos\theta_2 - T_{m1}\cos\theta_1 - F_p\sin\theta - F_w = 0 \quad (1)$$

$$T_{m2}\sin\theta_2 - T_{m1}\sin\theta_1 + F_p\cos\theta - 2T_c\sin(\Psi/2) = 0 \quad (2)$$

Upon substitution of terms, elimination of higher-order differentials, and the assumption that $\sin\Psi/2 = \Psi/2$ these equations reduce to the following:

$$\Delta(r\sigma_m\cos\theta) - rw_f\Delta s - pr\sin\theta\Delta s = 0 \quad (3)$$

$$\Delta(r\sigma_m\sin\theta) - \sigma_c\Delta s + pr\cos\theta\Delta s = 0 \quad (4)$$

Presented as Paper 78-314 at the AIAA 14th Annual Meeting and Technical Display, Washington, D.C., Feb. 7-9, 1978; submitted April 4, 1978; revision received Sept. 25, 1978.

Index categories: Lighter-than-Airships; Structural Design (including loads); Atmospheric and Space Sciences.

*Undergraduate. Student Member AIAA.

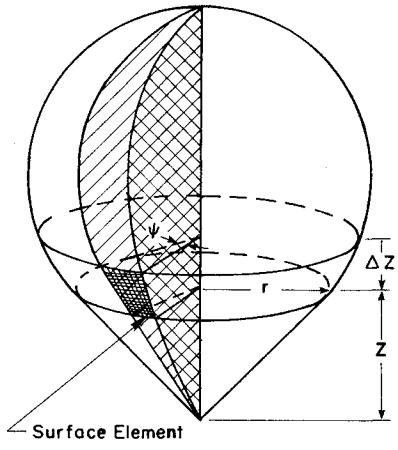

Fig. 1 Differential surface element.

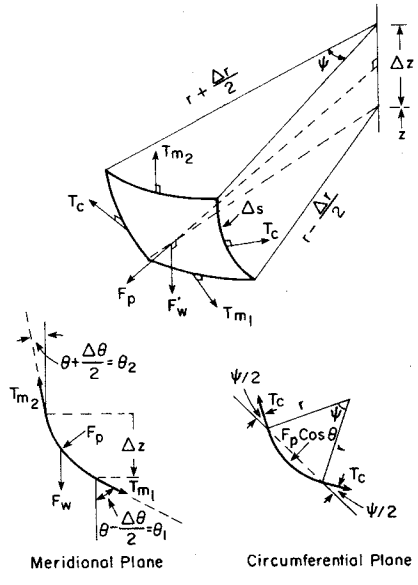

Fig. 2 Forces acting on film element.

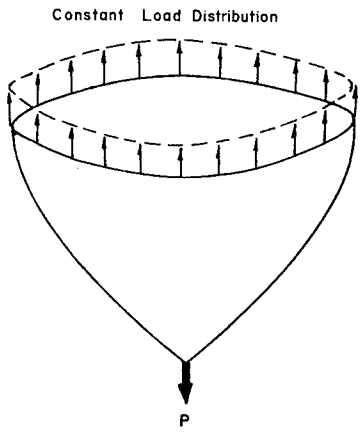

Fig. 3 Constant load distribution model.

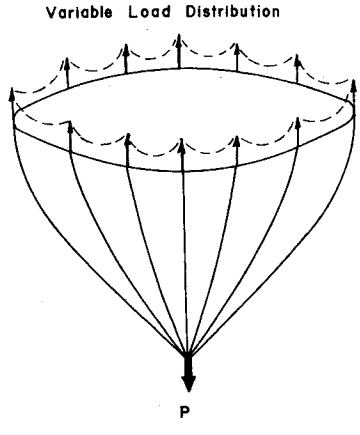

Fig. 4 Variable load distribution model.

These equations are further reduced after dividing by Δs and forming the derivative with respect to gore position, s, to become

$$\frac{d}{ds}(r\sigma_m\cos\theta) - rw_f - pr\sin\theta = 0 \tag{5}$$

$$\frac{d}{ds}(r\sigma_m\sin\theta) - \sigma_c + pr\cos\theta = 0 \tag{6}$$

Applying the chain rule to the derivatives results in the following:

$$\frac{d}{ds}(r\sigma_m)\cos\theta - (r\sigma_m)\sin\theta\frac{d\theta}{ds} - rw_f - pr\sin\theta = 0 \tag{7}$$

$$\frac{d}{ds}(r\sigma_m)\sin\theta + (r\sigma_m)\cos\theta\frac{d\theta}{ds} - \sigma_c + pr\cos\theta = 0 \tag{8}$$

These equations are then combined and rearranged with the additional assumption that the pressure differential p is proportional to the vertical distance from the zero pressure point a.

$$(r\sigma_m)\frac{d\theta}{ds} = \sigma_c\cos\theta - rw_f\sin\theta - br(z+a) \tag{9}$$

$$\frac{d}{ds}(r\sigma_m) = \sigma_c\sin\theta + rw_f\cos\theta \tag{10}$$

Four other differential equations can be written from geometric considerations of the balloon shape as follows:

$$\frac{dr}{ds} = \sin\theta \qquad \frac{dA}{ds} = 2\pi r \tag{11}$$

$$\frac{dz}{ds} = \cos\theta \qquad \frac{dV}{ds} = \pi r^2\cos\theta \tag{12}$$

These differential equations may be written in nondimensional form for greater convenience. This is done by introducing the nondimensional film weight parameter Σ_f along with the parameters λ and k to yield the final set of nondimensional differential equations:

$$(\bar{r}\bar{\sigma}_m)\theta' = \bar{\sigma}_c\bar{z}' - k\Sigma_f\bar{r}\bar{r}' - \bar{r}(\bar{z}+\bar{a}) \tag{13}$$

$$(\bar{r}\bar{\sigma}_m)' = \bar{\sigma}_c\bar{r}' + k\Sigma_f\bar{r}\bar{z}' \tag{14}$$

$$\bar{r}' = \sin \qquad \bar{A}' = 2\pi\bar{r} \tag{15}$$

$$\bar{z}' = \cos\theta \qquad \bar{V}' = \pi\bar{r}^2\bar{z}' \qquad \Sigma_f = w_f/kb\lambda \tag{16}$$

with differentiation with respect to $\bar{s}$ represented by the prime notation. These equations are solved simultaneously to yield a specific balloon shape for a given set of conditions.

This technique instituted by Smalley using these differential equations is generally used today for the majority of the balloon design work. This formulation assumes that the balloon is constructed of a continuous unbroken shell, and thus maintains a constant load disturbution as shown in Fig. 3. However, in reality these balloons are constructed of several gore sections. Along each seam between the gores a load tape is attached for reinforcement and load introduction purposes. This then alters the original assumption of a smooth continuous film. It is evident that the total load

carried by the balloon will be carried jointly between the film and the load tapes as shown in Fig. 4.

The relationship between the tape and film loadings at any meridional location can be defined by

$$P = F_t + F_f \tag{17}$$

where P is the total load carried by the balloon and F_t and F_f represent the tape and film loads, respectively.[3] The tape and film force can be expressed in terms of the tape and film strains according to the following equations:

$$F_t = nK_t\epsilon_t \tag{18}$$

$$F_f = \sigma_m 2\pi r = E_f\epsilon_f 2\pi r \tag{19}$$

This simplified relationship between film stresses and strain should be sufficiently accurate to evaluate the magnitude of the load distribution between tape and film. Combining these equations and assuming tape and film strains to be equal in the meridional direction yields

$$F_f = P[1 + (nK/2\pi rE_f)]^{-1} \tag{20}$$

If load tapes are not included in the theoretical model this equation would show that the entire load is carried in the balloon film. However, when typical values for the constants are substituted, this equation demonstrates that the film carries only about 40% of the total load.

For this reason Smalley's differential equations defining a balloon film and its associated loadings are reconsidered. The initial definition of the differential surface element is modified slightly in order to be used in this new formulation. The boundaries of the film element are still defined as shown previously, however, one meridional load tape is now included in the differential element under consideration. This is done with the understanding that integration around the balloon circumference will thus include all the load tapes:

$$T_{m1} = \left(r - \frac{\Delta r}{2}\right)\Psi\left(\sigma_m - \frac{\Delta\sigma_m}{2}\right) + \left(\epsilon_t - \frac{\Delta\epsilon_t}{2}\right)K_t \tag{21}$$

$$T_{m2} = \left(r + \frac{\Delta r}{2}\right)\Psi\left(\sigma_m + \frac{\Delta\sigma_m}{2}\right) + \left(\epsilon_t - \frac{\Delta\epsilon_t}{2}\right)K_t \tag{22}$$

and the weight force is rewritten as

$$F_w = w_f(r\Psi\Delta s) + w_t\Delta s \tag{23}$$

to include tape weight as well as film weight. It should be noted that the specific tape and film weights, w_t and w_f, are those corresponding to the undeformed condition. These modified weight and force terms are then included in the equilibrium equations. These equations are manipulated in a manner similar to the original Smalley derivations to yield the following differential equations:

$$\left(r\sigma_m + \frac{nK_t}{2\pi}\epsilon_t\right)\frac{d\theta}{ds} = \sigma_c\cos\theta - \sin\theta\left(rw_f + \frac{n}{2\pi}w_t\right) - br(z+a) \tag{24}$$

$$\frac{d}{ds}\left(r\sigma_m + \frac{nK_t}{2\pi}\epsilon_t\right) = \sigma_c\sin\theta + \cos\theta\left(rw_f + \frac{n}{2\pi}w_t\right) \tag{25}$$

The nondimensional forms of these two new equations can then be written using the nondimensional tape stiffness and weight parameters, $\bar{K}_t$ and Σ_t, as follows:

$$(\bar{r}\bar{\sigma}_m + k^3\bar{K}_t\epsilon_t)\theta' = \bar{\sigma}_c\bar{z}' - \bar{r}(\bar{z}+\bar{a}) - k^3\Sigma_t\bar{r}' - k\Sigma_f\bar{r}\bar{r}' \tag{26}$$

$$(\bar{r}\bar{\sigma}_m + k^3\bar{K}_t\epsilon_t)' = \bar{\sigma}_c\bar{r}' + (k\Sigma_f\bar{r} + k^3\Sigma_t)\bar{Z}' \tag{27}$$

$$\Sigma_t = nw_t/b\lambda^2 \qquad \bar{K}_t = nK_t/b\lambda^3 \tag{28}$$

The four differential equations describing the geometric balloon parameters from the original Smalley derivations remain unchanged. The solution of this set of equations then defines a balloon shape which realistically includes load tape effects.

A second consideration that would improve the existing design procedure involves film deformation and material properties. It would be advantageous to be able to define the meridional and circumferential film stresses in terms of the appropriate material properties and film strains. It is obvious that some material deformation does occur when the balloon fully deploys in the float configuration. By allowing for this material deformation in the design procedure, a more accurate estimation could be made of the actual film stress levels. This would also be beneficial in the balloon shape description. For this reason, the film stresses are defined as shown in the following nondimensional equations:

$$\bar{\sigma}_m = \bar{E}_m\epsilon_m + \bar{E}_{mc}\epsilon_c \tag{29}$$

$$\bar{\sigma}_c = \bar{E}_{mc}\epsilon_m + \bar{E}_c\epsilon_c \tag{30}$$

These equations incorporate the nondimensional material properties, $\bar{E}_{mc}, \bar{E}_c$, and $\bar{E}_m$ together with the meridional and circumferential film strains. This information concerning material properties and deformation together with the inclusion of load tapes in the theoretical model are added as modifications to the present design method. These improved design equations are then solved numerically by Gill's modification of the Runga-Kutta method.[4]

III. Numerical Evaluation

The differential equations derived from an investigation of a balloon surface element can be solved simultaneously using Gill's modified Runga-Kutta method to yield a specific balloon shape. This is done numerically with the aid of any of several computer programs designed specifically for this purpose.[4] Typically, these programs use the bottom of the balloon as a starting point for a solution. Assuming an initial angle θ_0, the set of equations is integrated over incremental gore positions until the apex of the balloon is reached. An existing balloon design program was modified to incorporate the proposed changes (i.e., inclusion of tape effects, material deformation, material properties) into the design procedure. An iterative technique added to the original program insures that the shape produced is for a flat-topped balloon ($\theta_{\text{final}} = -$

Table 1 Sample case parameters

Design parameters	
Float altitude, ft	120,000
Payload, lb	3,000
Specific bouyancy, lb/ft^3	3.455×10^{-4}
Normalizing length, ft	205.55
Film properties	
Thickness, in.	0.0008
Σ_f	0.10
E_f, psi	80×10^3
Poisson's ratio	0.5
E_m, E_c, psi	131.8
E_{mc}, psi	65.9
$\bar{E}_m, \bar{E}_c$	70.2
$\bar{E}_{mc}$	35.1
Load tape properties	
Number of tapes	150
Type	500 lb polyester
Tape stiffness, lb	1.5×10^4
Tape weight, lb/ft	0.00628
Σ_t	0.0646
$\bar{K}_t$	750

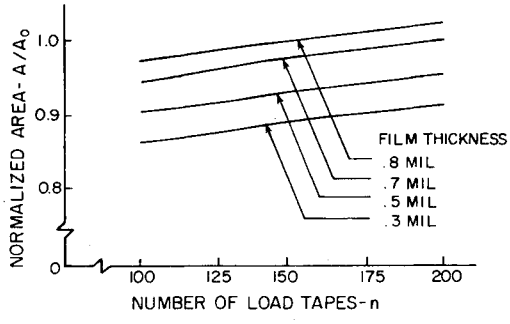

Fig. 5 Load tape effects on balloon shape.

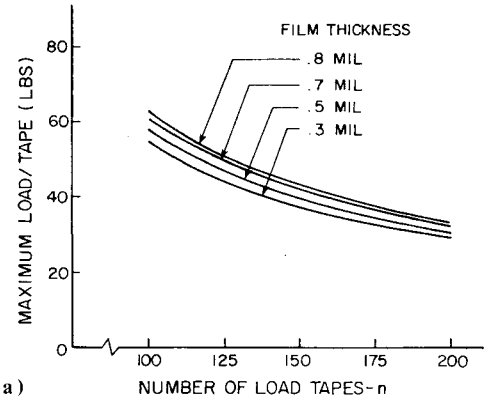

a)

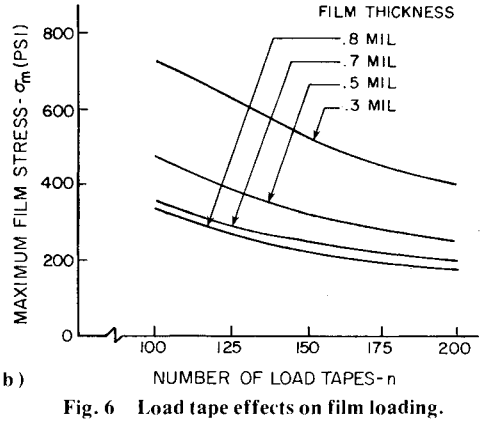

b)

Fig. 6 Load tape effects on film loading.

$\pi/2$). The solution at each gore position yields both an r and z value which eventually defines the entire balloon shape as shown in Fig. 1.

IV. Discussion of Results

For demonstration purposes a typical scientific mission was selected to evaluate the impact of load tapes and material properties (Table 1). Typical mission requirements involving a payload of 3000 lb floating at 120,000 ft are used for this evaluation. Several cases of various tape parameters were used to evaluate the influence of these quantities on the final balloon shape and stress distribution. The results of this study are presented in Figs. 5 and 6.

Considering the nondimensional tape parameters $\bar{K}_t$ and Σ_t, it is seen that a change in the number of tapes linearly affects each of these constants. Therefore, a change in n would essentially be the same as an appropriate change in the tape weight and stiffness. Allowing n to go to zero, the tape influence is completely negated, and the resulting design reverts back to the original method using a theoretical model with a uniform load distribution. This was done, and the results agreed to three significant figures with those reported by Smalley.[4] This check served to verify the validity of the newly modified design procedure.

The results presented in Figs. 5 and 6 clearly demonstrate the load tape effects on both the balloon shape and stress levels. As is true in most engineering situations, a tradeoff between two or more factors must be carefully considered in the design process. In this case the two design factors under consideration are tape weight and film weight. Obviously if the total weight of the system is reduced a smaller balloon would be acceptable. This would be directly reflected in a reduced manufacturing cost. Figure 5 shows that the smallest and least expensive balloon would result from the use of the thinnest film and fewest number of tapes possible in the construction process.

However, a most desirable combination of film thickness and number of tapes should be determined for the optimum balloon design. This selection process involves examining the loads which exist in both tapes and film. These loadings are presented in Fig. 6. It is seen that that tape loads are only slightly affected by a variation in film thickness. This indicates that the majority of the total system load is carried by the load tapes. It should be noted that manufacturing limitations with respect to maximum permissible gore width affect the total number of gores and thus the number of load tapes in any particular balloon. In this case the lowest possible number of gores is approximately 100. It is seen that the maximum load per tape is approximately 10% of the tape's rated load carrying capability. Thus, the critical factor in selecting the optimum tape-film combination becomes the loads experienced by the balloon film.

When investigating the stress levels present in the balloon film the nature of the film itself presents a major problem. If the balloon film could be characterized as a normal aerospace material with a well-defined yield stress, selection of the appropriate film thickness would be straightforward. Balloon film, however, is only a very thin piece of viscoelastic material with few well-defined stress characteristics. The problem is complicated further since the film must operate in an environment where presently the temperature and pressure can only be estimated. Therefore, the designer must compensate for these situations with large factors of safety in order to produce a reliable system. The results presented in Fig. 6 show that the same film stress level can be maintained using a smaller film thickness and more load tapes. This also results in a modest decrease in balloon surface area. These stresses are only a fraction of the stress normally assumed allowable. Even considering factors of safety to account for the nature of the balloon film these stress levels could be safely increased without sacrificing the structural integrity of the system.

V. Conclusions

The influence of tape weight and stiffness have been included in the design procedure for high-altitude scientific balloons. Typical accepted values of these parameters have been used to evaluate their influence on ballooon shape and stress distributions. It has been found that:

1) The total surface area of a balloon and its manufactured cost may be significantly reduced if the design were based on a film stress including load tape effects.

2) The total surface area of a balloon and its manufactured cost may be modestly reduced by simultaneously increasing the number of load tapes and reducing the film thickness.

3) Current design techniques result in factors of safety which may be unnecessarily large.

It is concluded that typical scientific balloons could be designed with significant size, weight, and cost reductions without compromising the structural integrity or reliability of the system by including the appropriate tape parameters. However, an accurate characterization of the film will be necessary before these changes will be an acceptable modification to the existing design process.

Acknowledgment

This work was supported by the Air Force Geophysics Laboratory, Air Force Systems Command, under Contract No. F19628-76-C-0082. The author also gratefully acknowledges the support and advice of J. L. Rand, Texas A&M University.

References

[1] Upson, R. H., "Evolution of Ballooning," *Scientific Ballooning Handbook*, Sec. I, NCAR-TN/1A-99, May 1975.

[2] Smalley, J. H., "Balloon Design Considerations," *Scientific Ballooning Handbook*, Sec. V, NCAR-TN/1A-99, May 1975.

[3] Alexander, H. and Agrawal, P., "Gore Panel Stress Analysis of High Altitude Balloons," Air Force Cambridge Research Laboratories, Hanson Air Force Base, Mass, AFCRL-TR-74-0597, Oct. 1974.

[4] Smalley, J. H., "Determination of the Shape of a Free Balloon," Air Force Cambridge Research Laboratories, Bedford, Mass., AFCRL-65-92, Feb. 1965.